water

MDPI

Article

Investigation of Geochemical Characteristics and Controlling Processes of Groundwater in a Typical Long-Term Reclaimed Water Use Area

Yong Xiao [1], Xiaomin Gu [1,*], Shiyang Yin [1,*], Xingyao Pan [2], Jingli Shao [1] and Yali Cui [1]

1 School of Water Resources and Environment, China University of Geosciences (Beijing), Beijing 100083, China; xiaoyong@cugb.edu.cn (Y.X.); jshao@cugb.edu.cn (J.S.); cuiyl@cugb.edu.cn (Y.C.)
2 Beijing Water Science and Technology Institute, Beijing 100044, China; water.china@aliyun.com
* Correspondence: cugbgxm@163.com (X.G.); yinshiyang1984@163.com (S.Y.); Tel.: +86-10-8232-2671 (X.G.); +86-10-8232-2671 (S.Y.)

Received: 5 August 2017; Accepted: 15 October 2017; Published: 18 October 2017

Abstract: The usage of reclaimed water can efficiently mitigate water crises, but it may cause groundwater pollution. To clearly understand the potential influences of long-term reclaimed water usage, a total of 91 samples of shallow and deep groundwater were collected from a typical reclaimed water use area during the dry and rainy seasons. The results suggest both shallow and deep groundwater are mainly naturally alkaline freshwater, which are composed mainly of Ca-HCO_3, followed by mixed types such as Ca-Na-HCO_3 and Ca-Mg-HCO_3. A seasonal desalination trend was observed in both shallow and deep aquifers due to dilution effects in the rainy season. Groundwater chemical compositions in both shallow and deep aquifers are still dominantly controlled by natural processes such as silicate weathering, minerals dissolution and cation exchange. Human activities are also the factors influencing groundwater chemistry. Urbanization has been found responsible for the deterioration of groundwater quality, especially in shallow aquifers, because of the relative thin aquitard. Reclaimed water usage for agricultural irrigation and landscape purposes has nearly no influences on groundwater quality in rural areas due to thick aquitards. Therefore, reclaimed water usage should be encouraged in arid and semiarid areas with proper hydrogeological condition.

Keywords: reclaimed water; hydrochemistry; water-rock interaction; anthropogenic contamination; groundwater

1. Introduction

Water scarcity has been a great threat to socioeconomic development as well as ecology in many parts of the world, especially in arid and semi-arid regions [1–4]. Due to the limited availability of surface water resources and precipitation, groundwater becomes the indispensable source of freshwater for various purposes such as drinking, irrigation and industry [5,6]. Long-term overexploitation has led to sharp decline of groundwater levels in many countries [7]. In order to alleviate shortages, non-conventional water resources such as wastewater and reclaimed water have been widely used for agricultural irrigation and as landscape water for decades [1,8,9].

However, wastewater and reclaimed water often have higher concentrations of major ions, heavy metals, nitrogen, phosphorus and other nutrients compared to freshwater [10]. Their usage may pose risks to environmental quality and human health [1]. Many researches have been conducted to reveal the potential influences of wastewater and reclaimed water usage on plants, soil and groundwater [2,9–15]. Generally, wastewater and reclaimed water usage can provide significant economic and ecological benefits [13]. Their reliable sources of nutrients can help to reduce the cost of fertilizer in agriculture and also increase the crop yield [16]. In addition, the usage of wastewater and reclaimed water in agriculture

can not only reduce the consumption of groundwater resource, but also increase groundwater recharge. However, negative effects are also observed. Salt, heavy metals and other pollutants tend to accumulate in soil with long-term wastewater and reclaimed water irrigation [17], and result in soil structure deterioration [18–20]. Moreover, heavy metals are found to potentially enrich in corps and pose health risk to humans [21,22]. Long-term irrigation with wastewater and reclaimed water also leads to pollutants transfer downward [23], threatening the groundwater quality and enhancing the complexity of groundwater chemistry governing mechanisms [9,12]. Therefore, understanding groundwater hydrogeochemical characteristics and their controlling factors in wastewater and reclaimed water used area is essential for managing and protecting groundwater quality and providing guidance for the usage of wastewater and reclaimed water.

Beijing, one of the cities in the world with the greatest water shortage, has used wastewater since the 1950s and reclaimed water since 2003. More than 2×10^8 m^3 of reclaimed water has been used for agricultural purpose since 2008 [12]. Reclaimed water is also widely used as landscape water to recover wetlands and dry rivers. Thus, it is necessary to get insight into the influences of their usage on groundwater. Considering the chemical composition of reclaimed water in Beijing [14,24], groundwater is potentially polluted by salt, nitrogen, heavy metals and organic pollutants. Previous research demonstrated that heavy metals and organic pollutants have low possibilities to constitute pollution to groundwater [14,17,25,26], but salt and nitrogen pollutants should be paid extra attention [12,27]. Although scholars have reported the spatial variation of groundwater quality in terms of salt and nitrogen pollutants [26,27], and also discussed the influences caused by the leakage of reclaimed water river on soil and groundwater quality in long-term wastewater and reclaimed water use areas in Beijing [9,14,15]. The regional groundwater hydrochemical characteristics and governing mechanisms are still poorly known. The objectives of this research are to investigate regional groundwater geochemical characteristics, and to address the controlling factors of groundwater chemistry in typical long-term reclaimed water use areas in Beijing.

2. Materials and Methods

2.1. Description of the Study Area

The study area is located in the southern part of the Beijing Plain, China (Figure 1). This area extends between longitudes of 116°13′–116°43′ E and latitudes of 39°26′–39°50′ N, encompassing an area of 1036 km^2. It belongs to a zone of temperate continental monsoon climate. The mean annual temperature is 11.6 °C. The mean annual precipitation 556 mm [28], with more than 70% occurring in the rainy season spanning June to September. While the mean annual potential evaporation is 1800 mm, which is more than three times of the mean annual precipitation.

The whole territory of the study area lies in the downstream part of the Yongding River alluvial-proluvial plain (Figure 1). The average elevation of this area ranges from 14 m to 52 m above sea level with the terrain gradually inclining along the northwest to southeast direction. Quaternary deposits formed by the alluvial-proluvial sediments of Yongding River are the main water-bearing media. Its thickness increases from 50 m to 300 m with the lithology changing from coarse sand to fine and sandy clay from northwest to southeast (Figure 2). A thick and continuous clay layer is observed at a depth of 100 m [29]. Groundwater above of this layer is regarded as shallow groundwater (SGW), and that below it is defined as deep groundwater (DGW). Groundwater regionally flows from northwest to southeast with its depth varying from 13 m to 35 m. The major recharge patterns are precipitation infiltration, lateral inflow, surface-water body leakage and irrigation infiltration. The main discharge components include lateral outflow and artificial abstraction.

The northern part of the study area, including Xihongmen, Jiugong, Yizhuang, Yinghai and Daxing (Figure 1), is mainly covered by urban land type, and other areas are covered by agricultural land type. There are two wastewater treatment plans (WTP), named Xiaohongmen WTP and Huangcun WTP, located in the study area. Due to the shortage of water resources, wastewater has been reused

for agricultural irrigation since the 1960s, and was gradually replaced by reclaimed water from the aforementioned WTP after 2003 [26]. Reclaimed water is also widely used for surface-water landscapes such as Niantan Park, the largest wetland park in the study area.

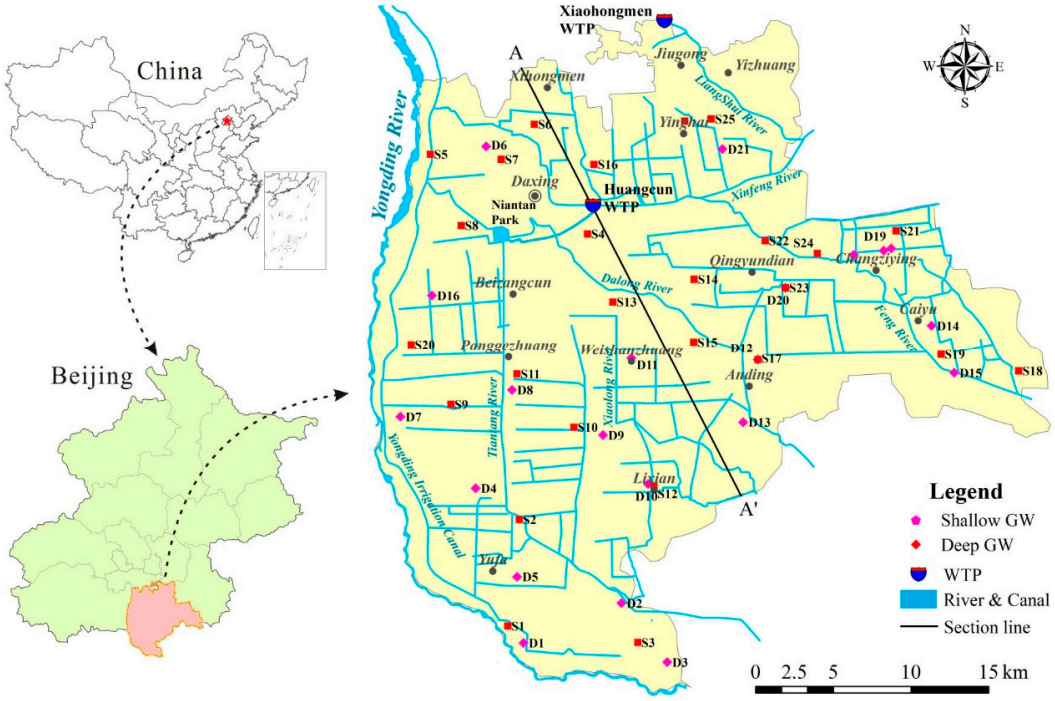

Figure 1. Location of the study area and sampling sites.

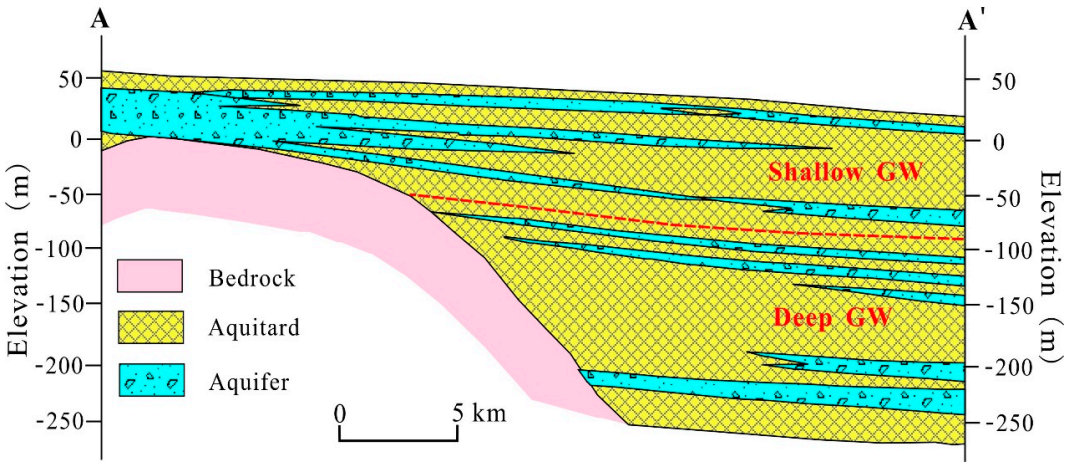

Figure 2. The hydrogeological cross section along the A-A'.

2.2. Sample Collection and Analysis

A total of 91 samples were collected from 26 SGW boreholes and 21 DGW boreholes in April (dry season) and September (rainy season) 2016. The locations of sampling sites were shown in Figure 1. All boreholes were pumped for more than 10 min to remove the stagnant water before sampling and field testing. Samples for laboratory analysis were collected in 2.5 L clean plastic bottles that had been thoroughly pre-washed with the water to be sampled. The temperature (T), electrical conductance (EC), total dissolved solids (TDS) and pH were measured on site using a multi-parameter device (Multi 350i/SET). The other chemical indices including cations (Na^+, K^+, Ca^{2+}, Mg^{2+}, NH_4^+) and

anions (Cl^-, SO_4^{2-}, HCO_3^-, NO_3^-, NO_2^-) were analyzed in the Laboratory of Groundwater Sciences and Engineering of the Institute of Hydrogeology and Environmental Geology, Chinese Academy of Geological Sciences. The laboratory analysis were conducted fallowing the analytical procedures described by Huang, et al. [30]. The ionic balance error of all samples were within a limit of ±5%.

3. Results and Discussion

3.1. Groundwater Chemistry

Groundwater chemistry involves enormous vital information on suitability for domestic, irrigational and industrial purposes [31], and is very helpful in understanding and identifying the processes governing the hydrochemical quality of groundwater [32,33]. Statistical summary of the hydrogeochemical data of both SGW and DGW during the dry and rainy seasons is presented in the Table 1.

As shown in Table 1, groundwater temperature ranges from 9.5 °C to 19.1 °C for SGW and between 12.5 °C and 18.1 °C for DGW during the dry season, and varies from 13.0 °C to 23.5 °C for SGW and between 15.5 °C and 22.5 °C for DGW during the rainy season. The temperature of groundwater presents a slight increase trend from the dry season to the rainy season. The pH values of both SGW and DGW in the study area are in the range of 7.1–8.0, indicating alkaline nature. The EC values of SGW varies from 585 μS/cm to 1716 μS/cm with an average of 1175 μS/cm during the dry season, and 547 μS/cm to 1794 μS/cm with an average of 1174 μS/cm during the rainy season. That of DGW ranges between 526 μS/cm and 1228 μS/cm with an average of 634 μS/cm, and from 531 μS/cm to 836 μS/cm with an average of 605 μS/cm. According to the classification of groundwater based on EC (fresh: <1500 μS/cm; brackish: 1500–3000 μS/cm; saline: >3000 μS/cm) [34], most of groundwater samples in the study area are fresh water, and only S2 and S17 fall under the brackish water category. The variation of EC shows a slight decrease trend for both SGW and DGW from the dry season to the rainy season. TDS values of SGW are in the range of 389–1140 mg/L, with an average of 782 mg/L during the dry season, and ranging between 547 mg/L to 1794 mg/L with an average of 792 mg/L during the rainy season. For the DGW, TDS values range from 309 mg/L to 800 mg/L with an average of 389 mg/L during the dry season, and between 298 mg/L and 554 mg/L with an average of 361 mg/L during the rainy season. The TDS values of DGW are lower than that of SGW during both seasons, indicating that the quality of DGW is better than that of SGW in term of the salinity. The seasonal variation of TDS for SGW is not significant, while that for DGW shows a slight decrease trend.

The average concentration of major ions during the dry season are in the following order: $Ca^{2+} > Na^+ > Mg^{2+} > K^+$ and $HCO_3^- > SO_4^{2-} > Cl^-$ for SGW, and $Na^+ > Ca^{2+} > Mg^{2+} > K^+$ and $HCO_3^- > SO_4^{2-} > Cl^-$ for DGW. The order changed to $Ca^{2+} > Mg^{2+} > Na^+ > K^+$ and $HCO_3^- > Cl^- > SO_4^{2-}$ for SGW, and $Ca^{2+} > Na^+ > Mg^{2+} > K^+$ and $HCO_3^- > SO_4^{2-} > Cl^-$ for DGW during the rainy season. All major ions for both SGW and DGW shows a seasonal variation of decrease. In addition, the content of NO_3^-, NO_2^- and NH_4^+ in SGW and DGW also presents a decrease trend from the dry season to the rainy season (Table 1). This seasonal decrease trend of cations and anions, which coincides with the seasonal variations of EC and TDS, is possibly the result of a dilution effect caused by fresh recharging water, mainly precipitation, in the rainy season [35].

As TDS is a comprehensive parameter reflecting major ion chemistry of groundwater [36], and nitrate is an important index indicating groundwater quality deterioration caused by anthropogenic sources [37], these two parameters are selected to explore the spatial variation of groundwater hydrochemistry. As displayed in Figure 3, TDS values of SGW are greater than that of DGW during both seasons. For SGW, the high values of TDS are mainly distributed at the northwest part of the study area, which is the urban area of Daxing District, Beijing, during both the dry and rainy seasons. In addition, S2 and S17 are found with relative high TDS values (>1000 mg/L) during both seasons. Compared to SGW, DGW has a relative low TDS value (all less than 800 mg/L) during the dry and rainy seasons. Apart from D3 in the south area, the relative high TDS values of DGW are found in

the northwest area, consistent with the high TDS values distribution area of SGW. All of the above suggests that urbanization is a factor impacting the groundwater chemistry.

Table 1. Statistical descriptions of chemical parameters in shallow and deep groundwater. Groundwater (GW); temperature (T); electrical conductance (EC); total dissolved solids (TDS).

Shallow GW	Dry Season					Rainy Season				
	Min	Max	Mean	SD [1]	C.V. (%) [2]	Min	Max	Mean	SD [1]	C.V. (%) [2]
T (°C)	9.5	19.1	14.7	2.7	18.08	13.0	23.5	19.5	2.8	14.53
pH	7.10	7.60	7.30	0.15	2.10	7.10	7.90	7.40	0.17	2.34
EC (μS/cm)	585	1716	1175	279	23.76	547	1794	1174	311	26.46
TDS (mg/L)	389	1140	782	208	26.54	337	1194	792	255	32.24
K (mg/L)	1.26	3.24	2.06	0.55	26.85	1.03	2.92	1.78	0.53	29.79
Na (mg/L)	20.4	196.0	89.7	36.0	40.19	13.6	104.0	53.2	24.6	46.13
Ca (mg/L)	38.9	172.0	103.6	35.1	33.85	40.1	172.0	105.5	37.0	35.07
Mg (mg/L)	16.9	135.0	60.7	25.3	41.68	17.0	130.0	58.5	22.7	38.79
Cl (mg/L)	11.0	302.0	107.1	64.4	60.10	17.6	280.0	86.4	61.0	70.59
SO_4 (mg/L)	25.5	261.0	110.8	67.2	60.64	28.5	186.0	93.1	50.6	54.38
HCO_3 (mg/L)	282.0	785.0	536.1	127.1	23.72	255.0	728.0	510.8	122.8	24.03
NO_3 (mg/L)	0.10	34.00	6.00	8.80	146.79	0.00	27.00	5.02	6.91	137.87
NO_2 (mg/L)	0.001	0.014	0.002	0.003	156.27	0.000	0.044	0.003	0.009	330.38
NH_4 (mg/L)	0.01	0.19	0.03	0.06	164.08	0.00	0.63	0.04	0.13	325.07
Deep GW	**Dry Season**					**Rainy Season**				
	Min	Max	Mean	SD [1]	C.V. (%) [2]	Min	Max	Mean	SD [1]	C.V. (%) [2]
T (°C)	12.5	18.1	15.3	1.7	11.08	15.5	22.5	19.1	2.2	11.29
pH	7.30	7.70	7.51	0.10	1.36	7.30	8.00	7.68	0.19	2.46
EC (μS/cm)	526	1228	634	167	26.33	531	836	605	76	12.53
TDS (mg/L)	309	800	389	118	30.33	298	554	361	54	14.97
K (mg/L)	1.23	2.84	1.97	0.43	21.66	1.02	3.75	1.57	0.66	42.16
Na (mg/L)	21.5	163.0	59.6	31.6	53.05	13.2	73.2	31.6	16.9	53.49
Ca (mg/L)	29.1	96.3	51.9	13.9	26.70	32.1	88.7	52.9	14.2	26.87
Mg (mg/L)	15.0	71.4	26.9	12.3	45.99	12.7	31.5	20.2	5.3	26.43
Cl (mg/L)	7.7	95.3	25.5	20.0	78.31	9.2	50.7	22.2	11.8	53.09
SO_4 (mg/L)	23.4	94.4	52.7	20.5	39.02	21.5	81.3	48.9	16.8	34.36
HCO_3 (mg/L)	206.0	650.0	328.1	111.8	34.06	227.0	348.0	284.1	31.0	10.92
NO_3 (mg/L)	0.10	7.41	1.27	1.59	125.13	0.01	5.35	1.13	1.22	107.92
NO_2 (mg/L)	0.001	0.005	0.001	0.001	129.04	0.001	0.003	0.001	0.001	92.47
NH_4 (mg/L)	0.01	0.18	0.02	0.04	186.24	0.01	0.10	0.02	0.03	129.04

Notes: [1] SD: Standard Deviation; [2] C.V. (%): Coefficient of Variation.

As presented in Figure 4, the high nitrate concentration of SGW and DGW during both seasons are distributed in the urban area northwest of the study area. Generally, natural nitrate concentration is lower than 10 mg/L, any value exceeding this is regarded as pollution caused by external factors [38]. Therefore, the chemistry of SGW at the northwest of the study area is influenced by the anthropogenic activities in some degree. Although, the highest nitrate concentration of DGW is lower than the geochemical limit (10 mg/L), the relative high nitrate values are located at the same regions with that of SGW, where the main urban part of the study area is located, indicating their anthropogenic sources of nitrogen.

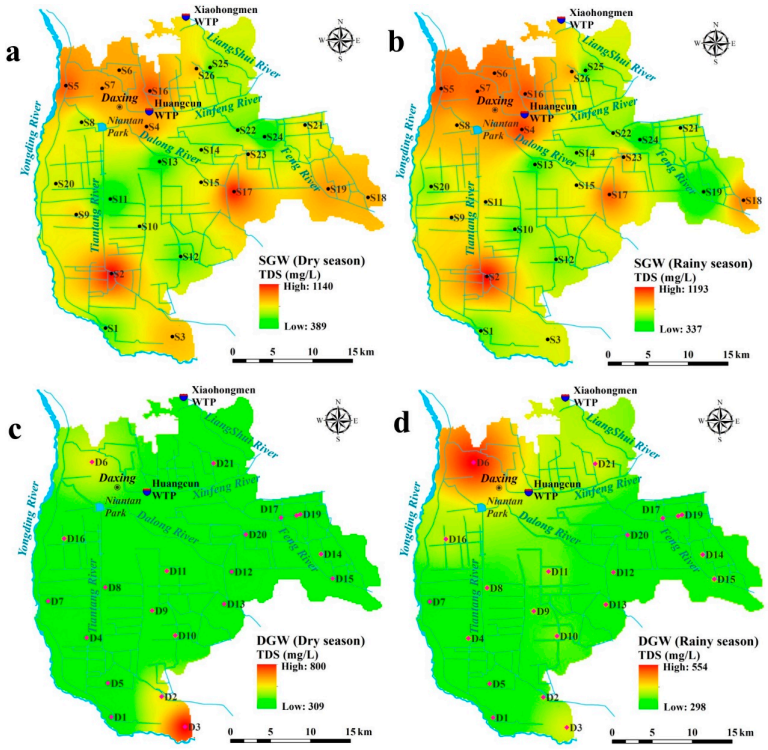

Figure 3. Spatial distribution of total dissolved solids (TDS). (**a**) shallow groundwater (SGW) during the dry season; (**b**) deep groundwater (DGW) during the dry season; (**c**) SGW during the rainy season; and (**d**) DGW during the rainy season.

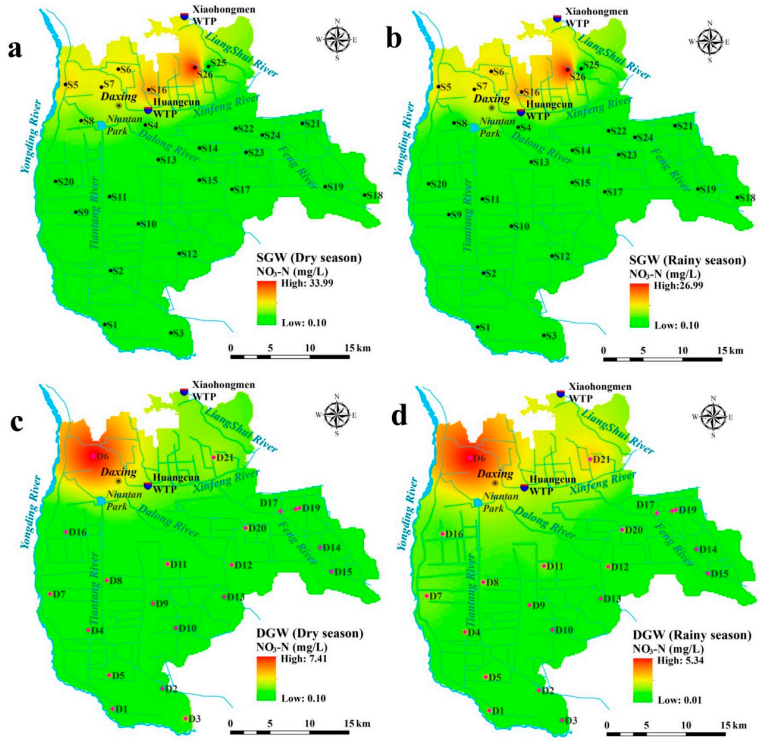

Figure 4. Spatial distribution of nitrate (NO_3-N). (**a**) shallow groundwater (SGW) during the dry season; (**b**) deep groundwater (DGW) during the dry season; (**c**) SGW during the rainy season; and (**d**) DGW during the rainy season.

3.2. Hydrogeochemical Facies

Piper diagram [39] has been introduced to understand the groundwater chemistry and identify hydrogeochemical facies in the study area. All groundwater samples, including both shallow and deep groundwater during the dry and rainy seasons, are plotted in Figure 5. The left ternary diagram of Figure 5 shows that about 58% and 69% of samples for SGW and DGW, to be of [Ca^{2+}] type, respectively; 35% and 2% of samples for SGW and DGW, were identified as [Mg^{2+}] type, respectively, and; 8% and 29% of samples for SGW and DGW, were of [Na^{+}] type, respectively. As indicated in the right ternary diagram, all the samples of both SGW and DGW are dominated by [HCO_3^{-}] type. Thus, groundwater in the study area is mainly Ca-HCO_3 type, followed by mixed types (including mixed Ca-Na-HCO_3 type and mixed Ca-Mg-HCO_3 type) (Figure 5).

To further understand the variation and distribution of groundwater chemical facies, water types of both SGW and DGW, during the dry and rainy seasons, are shown in Figure 6, and the percentages of each water type are summarized in Table 2. As seen in Figure 6, most of the area is dominated by Ca-HCO_3 type for both shallow and deep groundwater during the dry and rainy seasons.

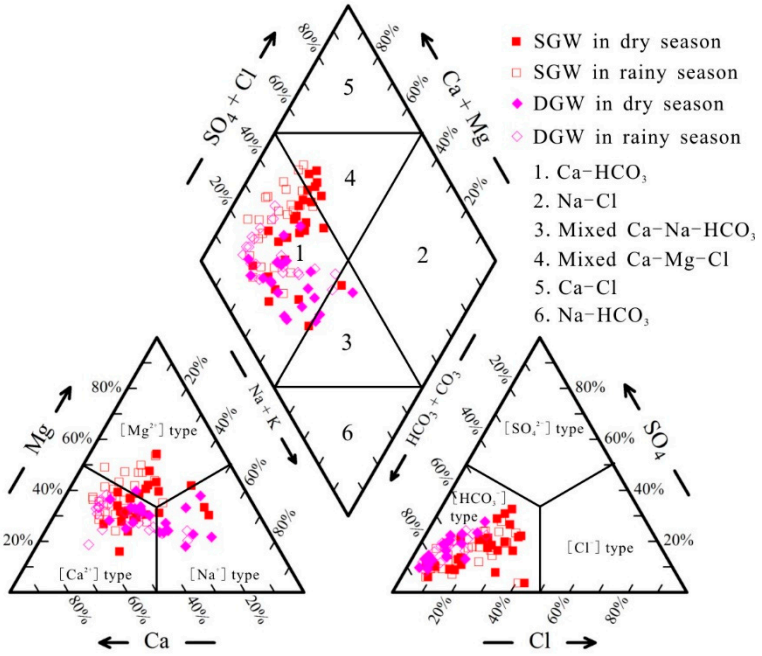

Figure 5. Piper diagram for both shallow and deep groundwater during the dry and rainy seasons.

For shallow groundwater, three and two hydrogeochemical facies are found during the dry and rainy seasons, respectively (Figure 6a,b). Ca-HCO_3 type water samples account 73.1% for the shallow groundwater during the dry season, and mixed Ca-Mg-Cl type water comes to the second with the percentage of 23.1%, followed by the mixed Ca-Na-HCO_3 type with the percentage of 3.85% (Table 2). The only one sample (S19) of mixed Ca-Na-HCO_3 type is found located in the eastern part of the study area. While all the mixed Ca-Mg-Cl type samples are located at the northwestern area, which is the urban area of Daxing District, Beijing. It seems that spatial variation of hydrogeochemical facies of shallow groundwater is related to land use type. Figure 6a,b also showed that hydrogeochemical facies changed from the dry season to the rainy season. The water of S19, which is of Ca-Na-HCO_3 type during the dry season, changed to be of Ca-HCO_3 type during the rainy season, while four out of the six mixed Ca-Mg-Cl type water changed to be of Ca-HCO_3 type. The only two remain mixed Ca-Mg-Cl type water are located at the downstream from the urban area of Daxing District. All of the above indicates that the quality of shallow groundwater evolves slightly fresher from the dry season to the rainy season.

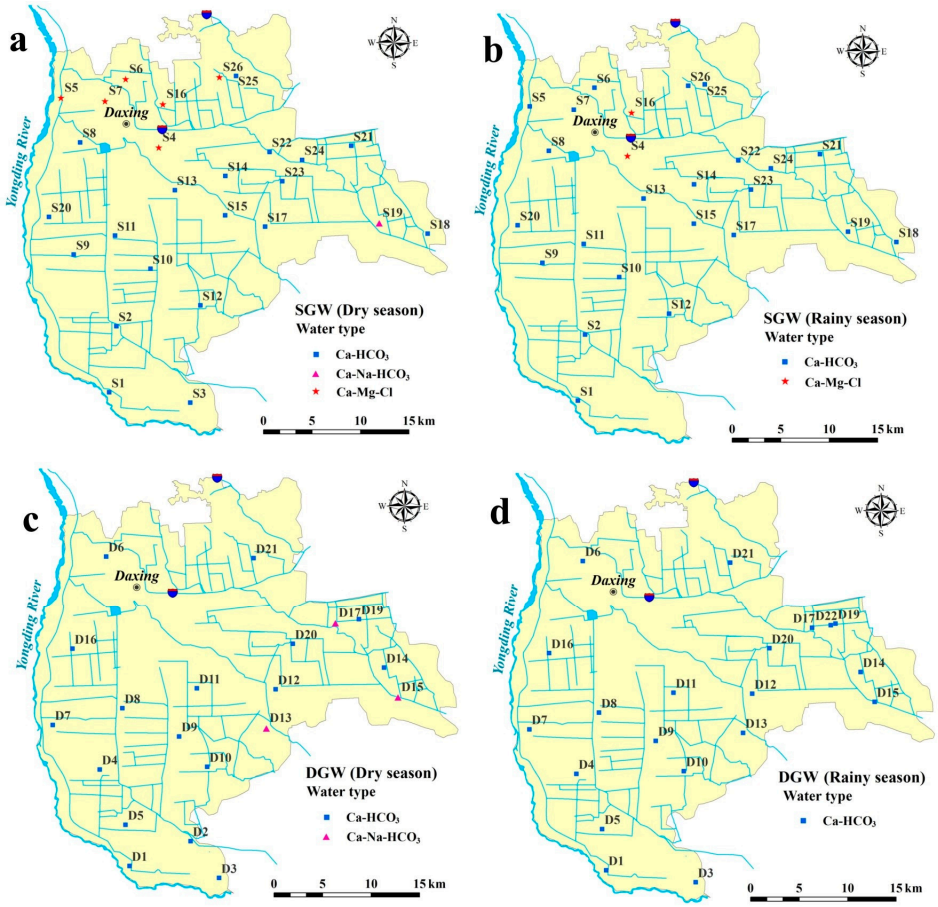

Figure 6. Distribution of water type. (**a**) shallow groundwater (SGW) during the dry season; (**b**) deep groundwater (DGW) during the dry season; (**c**) SGW during the rainy season; and (**d**) DGW during the rainy season.

Table 2. Percentage of different water types of shallow and deep groundwater.

Percent / Water Type	Shallow GW		Deep GW	
	Dry Season	Rainy Season	Dry Season	Rainy Season
$Ca\text{-}HCO_3$	73.08%	95.83%	85.00%	100.00%
Na-Cl				
Mixed $Ca\text{-}Na\text{-}HCO_3$	3.85%		15.00%	
Mixed Ca-Mg-Cl	23.08%	4.17%		
Ca-Cl				
$Na\text{-}HCO_3$				

As can been seen in Figure 6 and Table 2, the overall quality of DGW is better than that of SGW. During the dry season, about 85% of DGW samples are of $Ca\text{-}HCO_3$ type, and the other 15% of samples are of mixed $Ca\text{-}Na\text{-}HCO_3$ type. The $Ca\text{-}Na\text{-}HCO_3$ type water (D13, D15, D17) mainly distributes at the eastern part of the study area, which is basically consistent with the distributing area of $Ca\text{-}Na\text{-}HCO_3$ type water (S19) for SGW during the dry season. It is worth noting that the water type of DGW in the urban area is of $Ca\text{-}HCO_3$ type rather than mixed Ca-Mg-Cl type, indicating that the water type of DGW in the urban area has not significantly altered by the anthropogenic activities yet. Deep groundwater has similar seasonal variation tendency of hydrogeochemical facies with shallow groundwater. All of the three mixed Ca-Mg-Cl type water (D13, D15, D17) changed to the $Ca\text{-}HCO_3$

type water from the dry season to the rainy season. This change is possibly caused by the increase of the water recharge amount during the rainy season [40].

3.3. Mechanisms Controlling Groundwater Chemistry

3.3.1. Natural Factors

Gibbs diagrams, which are constructed by plotting ratios of $Na^+/Na^+ + Ca^{2+}$ and $Cl^-/(Cl^- + HCO_3^-)$ versus TDS [41], are widely used to identify natural processes, such as precipitation, rock-water interaction, evaporation/ crystallization, governing groundwater geochemistry [33,42,43]. As seen in Figure 7, all samples of both shallow and deep groundwater for both seasons are plotted in the rock dominance area, indicating that water-rock interaction is the main natural fundamental sources of groundwater chemical constituents in the study area. Evaporation was observed to have less contribution to the dissolved chemical constituents of groundwater during both dry and rainy seasons.

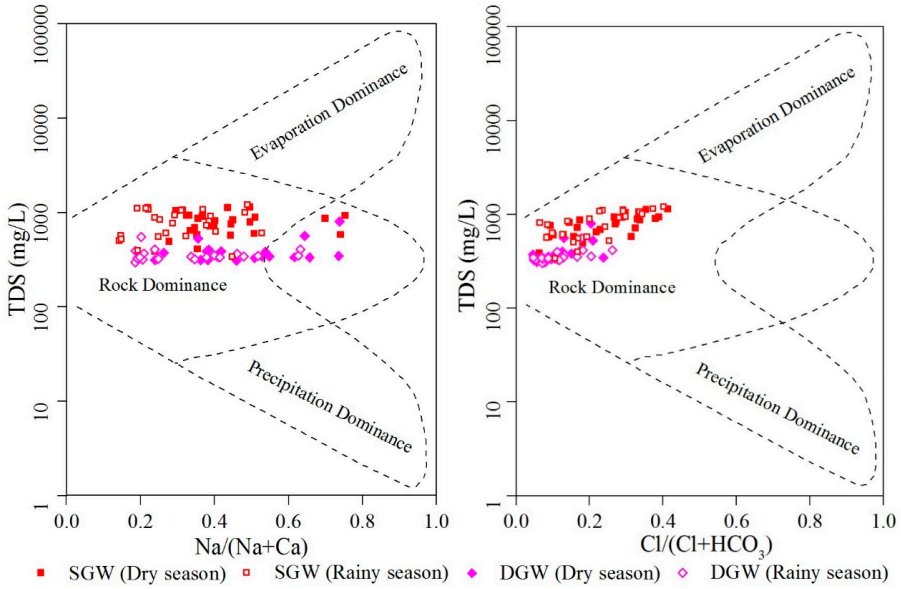

Figure 7. Gibbs diagrams showing the groundwater chemistry controlling mechanisms.

To further understand the details of rock water interaction in the study area, some ratio plots of major ions were conducted (Figure 8). The relation of Na^+ versus Cl^- of both shallow and deep groundwater for both seasons are demonstrated in Figure 8a. Generally, if Na^+ in groundwater is originated from the halite dissolution (1), then the molar ratio of Na^+/Cl^- should be approximately equal to 1. While if the ratio is greater than 1, Na^+ is mainly contributed by silicate weathering (2), whereas less than 1 indicates derivation from anthropogenic sources [43]. In this study, nearly all deep groundwater samples and most of the shallow groundwater samples during both seasons are with the ratio greater than 1, implying that silicate weathering (2) is an important source of sodium in shallow and deep groundwater [44]. Halite dissolution (1) is also one of the sources of sodium and chloride for both shallow and deep groundwater as some samples are observed with the ratio approximately equal to 1. This is confirmed by the Saturation Index (SI) of halite (Figure 9). In addition, it is worth to note that part of shallow groundwater samples are with the ratio less than 1, indicating the chemical constituents of shallow groundwater are contributed by anthropogenic sources in some degree.

$$NaCl \rightarrow Na^+ + Cl^- \quad (1)$$

$$2NaAlSi_3O_8 + 2CO_2 + 11H_2O \rightarrow 2Na^+ + Al_2Si_2O_5(OH)_4 + 3H_4SiO_4 + 2HCO_3^- \quad (2)$$

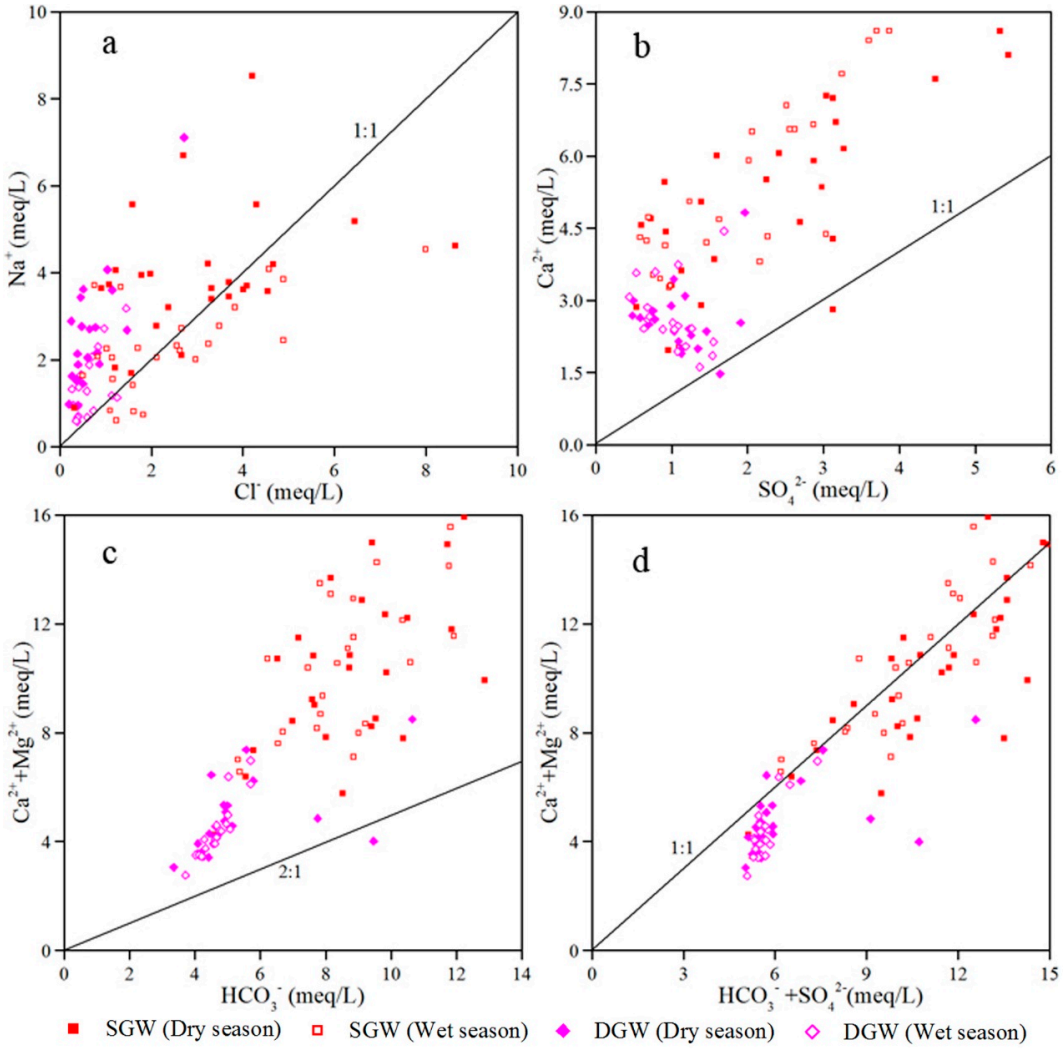

Figure 8. Scatter plots of different ions showing the correlation of major cations/anions to discriminate the geochemical processes. (**a**) Na^+ versus Cl^-; (**b**) Ca^{2+} versus SO_4^{2-}; (**c**) Ca^{2+}+Mg^{2+} versus HCO_3^-; and (**d**) Ca^{2+}+Mg^{2+} versus HCO_3^- + SO_4^{2-}.

The relation of Ca^{2+} and SO_4^{2-} is shown in Figure 8b. It is observed that Ca^{2+} increases with SO_4^{2-} in both shallow and deep groundwater, suggesting that these two ions may derive from the dissolution of gypsum and anhydrite (3, 4). The mineral equilibrium calculation results ($SI_{gypsum} < 1$, $SI_{anhydrite} < 1$) (Figure 9) indicate that all samples are under-saturated with the respect of gypsum and anhydrite, confirming the potential contributes of these two minerals dissolution. While the phenomenon that samples of both shallow and deep groundwater fall above the 1:1 line (Figure 8b), implying that Ca^{2+} and SO_4^{2-} are also included in some other different geochemical processes besides aforementioned processes [33].

$$CaSO_4 \rightarrow Ca^{2+} + SO_4^{2-} \quad (3)$$

$$CaSO_4 \cdot 2H_2O \rightarrow Ca^{2+} + SO_4^{2-} + 2H_2O \quad (4)$$

The relationship between Ca^{2+} + Mg^{2+} and HCO_3^- can reveal the source of calcium and magnesium of groundwater [33]. If the Ca^{2+} and Mg^{2+} only derive from the dissolution of carbonate, the (Ca^{2+} + Mg^{2+})/HCO_3^- molar ratio would be about 0.5. In this study, nearly all samples have higher ratios (>0.5) (Figure 8c), signifying the existence of additional sources of Ca^{2+} and Mg^{2+} and less contribution of Ca^{2+} and Mg^{2+} by carbonate dissolution [45]. This confirmed by the SI of calcite

and dolomite (Figure 9), showing that majority of the samples of both shallow and deep groundwater are over-saturated with respect to the calcite and dolomite.

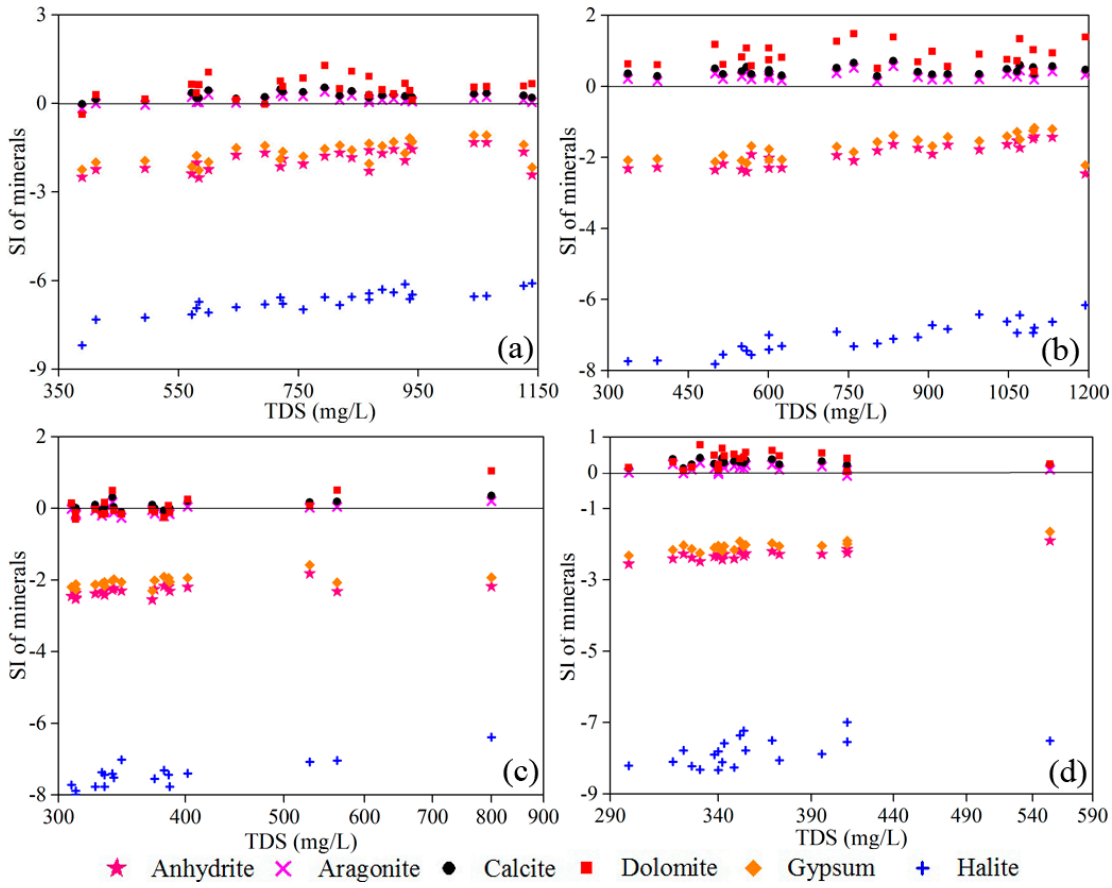

Figure 9. Saturation indices plots with selected minerals against TDS. (**a**) shallow groundwater (SGW) during the dry season; (**b**) deep groundwater (DGW) during the dry season; (**c**) SGW during the rainy season; and (**d**) DGW during the rainy season.

The diagram of (Ca^{2+} + Mg^{2+}) versus (HCO_3^- + SO_4^{2-}) were constructed to determine the mineralization processes (Figure 8d). The data that fall along the 1:1 line indicate contribution of dissolution of carbonates and sulfate minerals, and the data lying above and below the 1:1 line signify additional influences of the reverse cation-exchange process (5) and cation-exchange process (6), respectively [3]. As shown in Figure 8d, most of the data fall along the 1:1 line suggesting the weathering of carbonates and sulfate minerals. As discussed above, the contribution of carbonates weathering is less, so the dissolution of sulfate minerals (such as gypsum and anhydrite) is the main contribution. In addition, nearly all deep groundwater samples are observed to lie below the 1:1 line, suggesting the effects of cation-exchange process (6) on deep groundwater. However, some shallow groundwater samples fall above the equiline and some lie below the line, showing the contribution of the reverse cation-exchange process (5) and cation-exchange process (6) in the shallow groundwater in different area.

$$2Na^+ + CaX_2 \rightarrow Ca^{2+} + 2NaX \quad (5)$$

$$Ca^{2+} + 2NaX \rightarrow 2Na^+ + CaX_2 \quad (6)$$

Chloro-alkaline indices, including CAI-1 and CAI-2, were introduced to examine the influences of cation-exchange processes on groundwater chemistry (Figure 10). These two indices are expressed as Equations (7) and (8) (all ions are expressed in meq/L) [46]. The aforementioned indices would be

negative values if the hydrochemistry is dominantly affected by the normal cation-exchange process (6). On the other hand, if reverse cation-exchange process (5) takes place, these two indices would show positive values. Nearly all deep groundwater samples showed negative CAI (Figure 9), confirming the results of Figure 8d that cation-exchange process (6) occurs in deep groundwater. Some shallow groundwater samples are observed with negative CAI and others are with positive CAI, indicating cation-exchange process (6) and reverse cation-exchange process (5), respectively. This is consistent with the conclusion of Figure 8d.

$$\text{CAI} - 1 = \frac{\text{Cl}^- - \left(\text{Na}^+ + \text{K}^+\right)}{\text{Cl}^-} \quad (7)$$

$$\text{CAI} - 2 = \frac{\text{Cl}^- - \left(\text{Na}^+ + \text{K}^+\right)}{\text{HCO}_3^- + \text{SO}_4^{2-} + \text{CO}_3^- + \text{NO}_3^-} \quad (8)$$

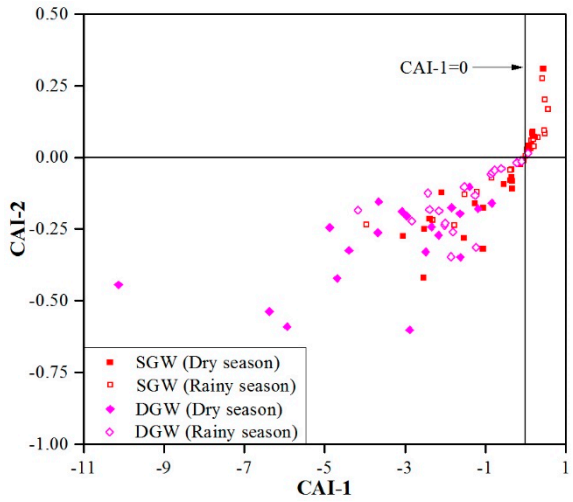

Figure 10. Scatter plot of chloro-alkaline indices CAI-1 vs. CAI-2.

3.3.2. Human Activities

The contributions of human activities to groundwater chemistry are complex and uncertain, and hard to determine [9,45]. Nitrate, which is mainly originated from multiple anthropogenic sources, is widely used to indicate the effects of human activities on groundwater chemistry [47,48]. In this study, the concentration of NO_3^- in sallow groundwater shows an increasing trend with the increase of Cl^- content (Figure 11a), indicating the similar sources of these two ions [49]. Cl^- is commonly derived from anthropogenic inputs as well as halite dissolution. Thus, the positive relation between NO_3^- and Cl^- signifies their anthropogenic inputs. This is also confirmed by the positive correlation of TDS with $(NO_3^- + Cl^-)/HCO_3^-$ (Figure 11b).

As can be seen in Figures 4 and 11, the high NO_3^- contents (exceeding geochemical limit 10 mg/L: S5, S6, S7, S16, S26) are only observed in shallow groundwater in the urban area during both seasons, implying that anthropogenic inputs such as domestic wastewater have a certain of influences on the chemistry of shallow groundwater in the urban area. This is also evidenced by the spatial distribution of water type of shallow groundwater (Figure 6a,b), of which Ca-Mg-Cl type for urban area while Ca-HCO_3 and Ca-Na-HCO_3 type for rural area. Urban anthropogenic wastes inputs are also found responsible for the relative higher NO_3^- content for the deep groundwater in the urban area (D6) in contrast with that in the rural area as the result of thin aquitards, but the influence is very limited. In the rural area (mainly agricultural area irrigated with reclaimed water), the nitrite content of shallow groundwater presents a poor correlation with the Cl^- (the Pearson correlation coefficient is 0.118 for

dry season and 0.383 for rainy season), suggesting human activities such as reclaimed water irrigation and reclaimed water river leakage have very limited influences on the shallow groundwater quality. This is possibly related to the thick aquitards above the water level. As a result, the NO_3^- contents of all shallow groundwater are below the geochemical limit 10 mg/L (Figure 11a). Deep groundwater in the rural area also have very low nitrite content (all below 10 mg/L). NO_3^- contents show nearly no variation with the increase of Cl^- contents (Figure 11), demonstrating that the chemistry of deep groundwater in the rural area is not affected by anthropogenic pollutions.

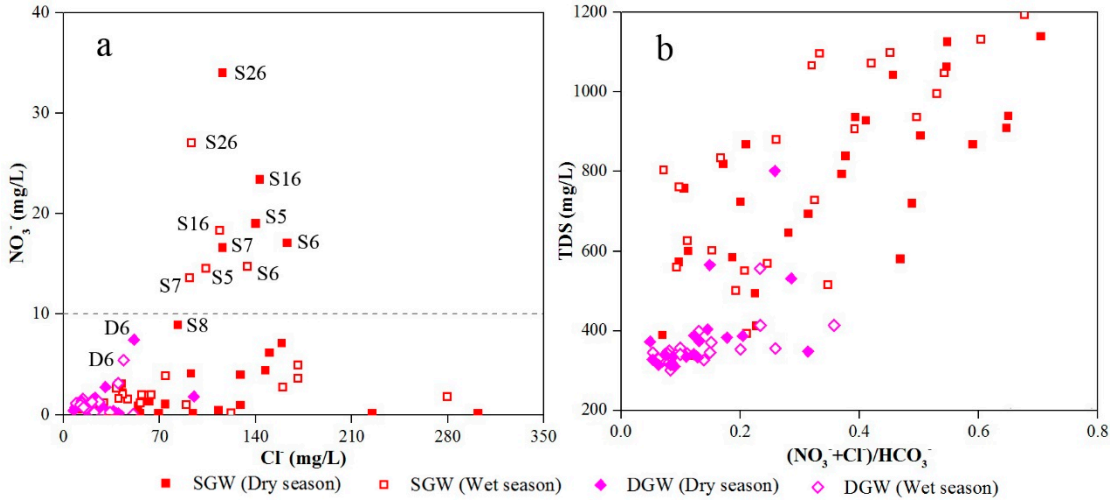

Figure 11. Scatter plot of (**a**) NO_3^- versus Cl^-; and (**b**) TDS versus $(NO_3^- + Cl^-)/HCO_3^-$.

4. Conclusions

Reclaimed water has been widely used in many arid and semi-arid regions around the world to mitigate water crises. In the present study, hydrogeochemical characteristics of groundwater in a long-term reclaimed water use area in Beijing were investigated, and the controlling processes of groundwater chemistry were also discussed in detail. The summarized conclusions are as follows.

Groundwater, including shallow groundwater and deep groundwater, is mainly naturally alkaline freshwater in the study area. The average concentration of all ions in deep aquifers are lower than that in shallow aquifers throughout the year, resulting in fresher and better quality deep groundwater. Moreover, the values of most indices of groundwater decrease from the dry season to the rainy season in both shallow and deep aquifers as the results of dilute effects in the rainy season. In terms of hydrogeochemical facies, both shallow groundwater and deep groundwater are mainly Ca-HCO_3 type, followed by mixed types such as mixed Ca-Na-HCO_3 type and mixed Ca-Mg-HCO_3 type. The hydrogeochemical facies of both shallow and deep groundwater were observed with a desalination change that water types evolved from mixed types in the dry season to Ca-HCO_3 type in the rainy season.

The chemistry of groundwater in the study area is affected by natural processes as well as human activities. Water-rock interactions such as dissolutions of silicate, halite, gypsum, anhydrite and cation exchange are the dominant natural processes controlling the chemical composition of groundwater in both aquifers and both seasons. While the influences of human activities is related to the hydrogeological condition. The urban area with the thin aquitard is observed as having obvious influences of anthropogenic inputs on groundwater chemistry, especially for shallow aquifers, while the existence of thick aquitards in rural areas greatly reduces or even eliminates the potential negative effects of reclaimed water usage on groundwater chemistry. Thus, hydrogeological condition should be taken into account when using reclaimed water for agricultural irrigation and landscape purpose.

Acknowledgments: This research was supported by the Fundamental Research Funds for the Central Universities (No. 2652016022), the National Key R&D Program of China (2017YFC0406106) and the Ministry of Water Resources public projects (No. 201101051). The authors would like to express their Sincere thanks to the Anonymous reviewers for their invaluable comments on the manuscript.

Author Contributions: Shiyang Yin, Jingli Shao and Yali Cui conceived and designed the research; Shiyang Yin, Xiaomin Gu, Yong Xiao and Xingyao Pan performed the field works and data collection; Yong Xiao and Xiaomin Gu analyzed the data; Yong Xiao wrote the paper. All authors read and approved the final manuscript.

Conflicts of Interest: The authors declare no conflicts of interest.

References

1. Elgallal, M.; Fletcher, L.; Evans, B. Assessment of potential risks associated with chemicals in wastewater used for irrigation in arid and semiarid zones: A review. *Agric. Water Manag.* **2016**, *177*, 419–431. [CrossRef]
2. Lu, S.; Zhang, X.; Liang, P. Influence of drip irrigation by reclaimed water on the dynamic change of the nitrogen element in soil and tomato yield and quality. *J. Clean. Prod.* **2016**, *139*, 561–566. [CrossRef]
3. Wang, L.; Dong, Y.; Xie, Y.; Song, F.; Wei, Y.; Zhang, J. Distinct groundwater recharge sources and geochemical evolution of two adjacent sub-basins in the lower shule river basin, northwest China. *Hydrogeol. J.* **2016**, *24*, 1967–1979. [CrossRef]
4. Gu, X.; Xiao, Y.; Yin, S.; Shao, J.; Pan, X.; Niu, Y.; Huang, J. Groundwater level response to hydrogeological factors in a semi-arid basin of Beijing, China. *J. Water Supply: Res. Technol. AQUA* **2017**, *66*, 266–278. [CrossRef]
5. Esmaeili-Vardanjani, M.; Rasa, I.; Amiri, V.; Yazdi, M.; Pazand, K. Evaluation of groundwater quality and assessment of scaling potential and corrosiveness of water samples in Kadkan aquifer, Khorasan-e-Razavi Province, Iran. *Environ. Monit. Assess.* **2015**, *187*, 53. [CrossRef] [PubMed]
6. Xiao, Y.; Gu, X.; Yin, S.; Shao, J.; Cui, Y.; Zhang, Q.; Niu, Y. Geostatistical interpolation model selection based on ArcGIS and spatio-temporal variability analysis of groundwater level in piedmont plains, northwest China. *SpringerPlus* **2016**, *5*, 425. [CrossRef] [PubMed]
7. Zhou, Y.; Xiao, W.; Wang, J.; Zhao, Y.; Huang, Y.; Tian, J.; Chen, Y. Evaluating spatiotemporal variation of groundwater depth/level in Beijing plain, a groundwater-fed area from 2001 to 2010. *Adv. Meteorol.* **2016**, *2016*, 8714209. [CrossRef]
8. Akponikp, P.I.; Wima, K.; Yacouba, H.; Mermoud, A. Reuse of domestic wastewater treated in macrophyte ponds to irrigate tomato and eggplant in semi-arid West-Africa: Benefits and risks. *Agric. Water Manag.* **2011**, *98*, 834–840. [CrossRef]
9. Yu, Y.; Song, X.; Zhang, Y.; Zheng, F.; Ji, L.; Liu, L. Identifying spatio-temporal variation and controlling factors of chemistry in groundwater and river water recharged by reclaimed water at Huai River, North China. *Stoch. Environ. Res. Risk Assess.* **2014**, *28*, 1135–1145. [CrossRef]
10. Tunc, T.; Sahin, U. The changes in the physical and hydraulic properties of a loamy soil under irrigation with simpler-reclaimed wastewaters. *Agric. Water Manag.* **2015**, *158*, 213–224. [CrossRef]
11. Al Kuisi, M.; Aljazzar, T.; Rüde, T.; Margane, A. Impact of the use of reclaimed water on the quality of groundwater resources in the Jordan Valley, Jordan. *CLEAN Soil Air Water* **2008**, *36*, 1001–1014. [CrossRef]
12. Shang, F.; Ren, S.; Yang, P.; Li, C.; Xue, Y.; Huang, L. Modeling the risk of the salt for polluting groundwater irrigation with recycled water and ground water using HYDRUS-1 D. *Water Air Soil Pollut.* **2016**, *227*, 189. [CrossRef]
13. Wu, W.; Yin, S.; Liu, H.; Niu, Y.; Bao, Z. The geostatistic-based spatial distribution variations of soil salts under long-term wastewater irrigation. *Environ. Monit. Assess.* **2014**, *186*, 6747–6756. [CrossRef] [PubMed]
14. Yin, S.; Wu, W.; Liu, H.; Zhe, B. The impact of river infiltration on the chemistry of shallow groundwater in a reclaimed water irrigation area. *J. Contam. Hydrol.* **2016**, *193*, 1–9. [CrossRef] [PubMed]
15. Yu, Y.; Song, X.; Zhang, Y.; Zheng, F.; Liang, J.; Han, D.; Ma, Y. Identification of key factors governing chemistry in groundwater near the water course recharged by reclaimed water at Miyun County, Northern China. *J. Environ. Sci.* **2013**, *25*, 1754–1763. [CrossRef]
16. Rosenqvist, H.; Dawson, M. Economics of using wastewater irrigation of willow in Northern Ireland. *Biomass Bioenergy* **2005**, *29*, 83–92. [CrossRef]
17. Bao, Z.; Wu, W.; Liu, H.; Chen, H.; Yin, S. Impact of long-term irrigation with sewage on heavy metals in soils, crops, and groundwater—A case study in Beijing. *Pol. J. Environ. Stud.* **2014**, *23*, 309–318.

18. Adhikari, P.; Shukla, M.K.; Mexal, G.J. Spatial variability of hydraulic conductivity and sodium content of desert soils: Implications for management of irrigation using treated wastewater. *Trans. ASABE* **2012**, *55*, 1711–1721. [CrossRef]
19. Goncharenko, A.M.; Garanovich, I.L. Impact of field application of treated wastewater on hydraulic properties of vertisols. *Water Air Soil Pollut.* **2007**, *184*, 347–353.
20. Qadir, M.; Wichelns, D.; Raschid-Sally, L.; Mccornick, P.G.; Drechsel, P.; Bahri, A.; Minhas, P.S. The challenges of wastewater irrigation in developing countries. *Agric. Water Manag.* **2010**, *97*, 561–6568. [CrossRef]
21. Kalavrouziotis, I.K.; Koukoulakis, P.H.; Papadopoulos, A.H.; Mehra, A. Heavy metal accumulation in brussels sprouts after irrigation with treated municipal waste water. *J. Plant Interact.* **2009**, *4*, 41–48. [CrossRef]
22. Khan, S.; Cao, Q.; Zheng, Y.M.; Huang, Y.Z.; Zhu, Y.G. Health risks of heavy metals in contaminated soils and food crops irrigated with wastewater in Beijing, China. *Environ. Pollut.* **2008**, *152*, 686–692. [CrossRef] [PubMed]
23. Xu, J.; Wu, L.S.; Chang, A.C.; Zhang, Y. Impact of long-term reclaimed wastewater irrigation on agricultural soils: A preliminary assessment. *J. Hazard. Mater.* **2010**, *183*, 780–786. [CrossRef] [PubMed]
24. Wu, W. Research on Groundwater Vulnerability Experiment of Reclaimed Wastewater District and Irrigation Allocation. Ph.D. Thesis, China University of Geosciences (Beijing), Beijing, China, 2009.
25. Bao, Z.; Wu, W.; Liu, H.; Yin, S.; Chen, H. Geostatistical analyses of spatial distribution and origin of soil nutrients in long-term wastewater-irrigated area in beijing, china. *Acta Agric. Scand. Sect. B Soil Plant Sci.* **2014**, *64*, 235–243. [CrossRef]
26. Wang, S.; Wu, W.; Liu, F.; Yin, S.; Bao, Z.; Liu, H. Spatial distribution and migration of nonylphenol in groundwater following long-term wastewater irrigation. *J. Contam. Hydrol.* **2015**, *177–178*, 85–92. [CrossRef] [PubMed]
27. Niu, Y.; Yin, S.; Liu, H.; Wu, W.; Li, B. Use of geostatistics to determine the spatial variation of groundwater quality: A case study in Beijing's reclaimed water irrigation area. *Pol. J. Environ. Stud.* **2015**, *24*, 611–618.
28. Zhang, X.; Sun, M.; Wang, N.; Huo, Z.; Huang, G. Risk assessment of shallow groundwater contamination under irrigation and fertilization conditions. *Environ. Earth Sci.* **2016**, *75*, 603. [CrossRef]
29. Li, S.; Wang, X.; Zhou, J.; Tang, X.; Wang, Z. Distribution law of high fluoride groundwater in quaternary in daxing district of Beijing. *Geoscience* **2012**, *26*, 407–414.
30. Huang, G.; Chen, Z.; Liu, F.; Sun, J.; Wang, J. Impact of human activity and natural processes on groundwater arsenic in an urbanized area (South China) using multivariate statistical techniques. *Environ. Sci. Pollut. Res.* **2014**, *21*, 13043–13054. [CrossRef] [PubMed]
31. Alam, F. Evaluation of hydrogeochemical parameters of groundwater for suitability of domestic and irrigational purposes: A case study from central ganga plain, India. *Arab. J. Geosci.* **2014**, *7*, 4121–4131. [CrossRef]
32. Li, P.; Wu, J.; Qian, H. Hydrochemical appraisal of groundwater quality for drinking and irrigation purposes and the major influencing factors: A case study in and around Hua County, China. *Arab. J. Geosci.* **2016**, *9*, 15. [CrossRef]
33. Nematollahi, M.J.; Ebrahimi, P.; Razmara, M.; Ghasemi, A. Hydrogeochemical investigations and groundwater quality assessment of Torbat-Zaveh plain, Khorasan Razavi, Iran. *Environ. Monit. Assess.* **2016**, *188*, 2. [CrossRef] [PubMed]
34. Saxena, V.K.; Singh, V.S.; Mondal, N.C.; Jain, S.C. Use of hydrochemical parameters for the identification of fresh groundwater resources, Potharlanka Island, India. *Environ. Geol.* **2003**, *44*, 516–521. [CrossRef]
35. Zhai, Y.; Wang, J.; Zhang, Y.; Teng, Y.; Zuo, R.; Huan, H. Hydrochemical and isotopic investigation of atmospheric precipitation in Beijing, China. *Sci. Total Environ.* **2013**, *456–457*, 202–211. [CrossRef] [PubMed]
36. Wagh, V.M.; Panaskar, D.B.; Varade, A.M.; Mukate, S.V.; Gaikwad, S.K.; Pawar, R.S.; Muley, A.A.; Aamalawar, M.L. Major ion chemistry and quality assessment of the groundwater resources of nanded tehsil, a part of Southeast Deccan Volcanic Province, Maharashtra, India. *Environ. Earth Sci.* **2016**, *75*, 1418. [CrossRef]
37. Esmaeili, A.; Moore, F.; Keshavarzi, B. Nitrate contamination in irrigation groundwater, Isfahan, Iran. *Environ. Earth Sci.* **2014**, *72*, 2511–2522. [CrossRef]
38. Karagüzel, R.; Irlayici, A. Groundwater pollution in the Isparta Plain, Turkey. *Environ. Geol.* **1998**, *34*, 303–308. [CrossRef]

39. Piper, A. A graphic procedure in the geochemical interpretation of water analysis. *Eos Trans. Am. Geophys. Union* **1944**, *25*, 914–928. [CrossRef]
40. Zhai, Y.; Lei, Y.; Zhou, J.; Li, M.; Wang, J.; Teng, Y. The spatial and seasonal variability of the groundwater chemistry and quality in the exploited aquifer in the Daxing District, Beijing, China. *Environ. Monit. Assess.* **2015**, *187*, 43. [CrossRef] [PubMed]
41. Gibbs, R.J. Mechanisms controlling world water chemistry. *Science* **1970**, *170*, 1088–1090. [CrossRef] [PubMed]
42. Xiao, Y.; Shao, J.; Cui, Y.; Zhang, G.; Zhang, Q. Groundwater circulation and hydrogeochemical evolution in Nomhon of Qaidam Basin, Northwest China. *J. Earth Syst. Sci.* **2017**, *126*, 26. [CrossRef]
43. Kanagaraj, G.; Elango, L. Hydrogeochemical processes and impact of tanning industries on groundwater quality in Ambur, Vellore District, Tamil Nadu, India. *Environ. Sci. Pollut. Res. Int.* **2016**, *23*, 24364–24383. [CrossRef] [PubMed]
44. Farid, I.; Zouari, K.; Rigane, A.; Beji, R. Origin of the groundwater salinity and geochemical processes in detrital and carbonate aquifers: Case of Chougafiya Basin (central Tunisia). *J. Hydrol.* **2015**, *530*, 508–532. [CrossRef]
45. Li, P.; Zhang, Y.; Yang, N.; Jing, L.; Yu, P. Major ion chemistry and quality assessment of groundwater in and around a mountainous tourist town of China. *Expo. Health* **2016**, *8*, 239–252. [CrossRef]
46. Schoeller, H. Qualitative evaluation of groundwater resources. In *Methods and Techniques of Groundwater Investigations and Development*; The United Nations Educational, Scientific and Cultural Organization (UNESCO): Paris, France, 1965; pp. 54–83.
47. Abdesselem, K.; Azedine, H.; Lynda, C. Groundwater hydrochemistry and effects of anthropogenic pollution in Béchar city (SW Algeria). *Desalin. Water Treat.* **2015**, *57*, 14034–14043. [CrossRef]
48. Patel, P.; Raju, N.J.; Reddy, B.C.S.R.; Suresh, U.; Gossel, W.; Wycisk, P. Geochemical processes and multivariate statistical analysis for the assessment of groundwater quality in the Swarnamukhi River Basin, Andhra Pradesh, India. *Environ. Earth Sci.* **2016**, *75*, 611. [CrossRef]
49. Marghade, D.; Malpe, D.B.; Zade, A.B. Major ion chemistry of shallow groundwater of a fast growing city of central India. *Environ. Monit. Assess.* **2012**, *184*, 2405–2418. [CrossRef] [PubMed]